Sidewall Suppression and Top Surface Enhancement of Light Extraction Efficiency in Vertically Stacked Full-Color Micro-LEDs Based on L-Shaped

N.B. When citing this work, cite the original published paper.

(article starts on next page)

Sidewall Suppression and Top Surface Enhancement of Light Extraction Efficiency in Vertically Stacked Full-Color Micro-LEDs Based on L-Shaped Metal Walls

Huachang Guo, Jun He, Jie Sun,* Kaixin Zhang,* Zhonhang Huang, Tailiang Guo, Qun Yan, Victor Belyaev, Aslan Abduev, and Alexander Kazak

Micro light-emitting diodes (Micro-LEDs) are regarded as the core of next-generation display technology due to their high brightness and energy efficiency. However, the reduction in the size of Micro-LEDs has led to increased manufacturing challenges and exacerbated issues such as sidewall emission, which hinder the development of high-pixel-density displays. This paper proposes a vertically stacked Micro-LED design based on an L-shaped metal wall structure, aiming to suppress sidewall emission and enhance top light extraction efficiency (LEE). Through parameter scanning, the dimensions of the Micro-LED and the thickness of the epitaxial layer are optimized. Combined with inclined sidewalls and the reflective structure of the L-shaped metal wall, the optical characteristics of red, green, and blue Micro-LEDs are analyzed using ray-tracing simulations. The sidewall emission is significantly reduced (with a maximum reduction of 68.04% compared to vertically stacked Micro-LEDs without metal walls), and top light emission is enhanced (the LEE within ±90° direction for blue, green, and red light increased by 196.18%, 51.69%, and 3.45%, respectively, compared to stacked Micro-LEDs without metal walls). The simulation results demonstrate the potential of the L-shaped metal wall in vertically stacked full-color Micro-LED displays, providing a new approach to suppressing optical crosstalk and improving display performance.

1. Introduction

Micro light-emitting diodes (Micro-LEDs) are increasingly regarded as a key technology for future displays due to their advantages such as high brightness, long lifespan, fast response time, and ultra-high resolution.[1–3] Micro-LEDs have a wide range of applications, including wearable devices, augmented reality, virtual reality, microprojectors, high-resolution televisions, maskless photolithography and optical communication.[4–9] Traditional display technologies, such as liquid crystal displays and organic light-emitting diodes (OLEDs), have achieved significant success in the market. However, they still face limitations in brightness, energy efficiency, and lifespan.[10] In contrast, Micro-LEDs not only offer higher energy efficiency but also enable faster response times, making them highly advantageous for high dynamic range and high refresh rate displays.[11] Despite their superior performance, the commercialization of Micro-LEDs faces several challenges, particularly in achieving full-color displays and high pixel density.

Full-color Micro-LED displays are primarily realized through two methods: quantum dot color conversion[12–14] and the combination of red, green, and blue (RGB) primary colors.[15] Quantum dot color conversion technology utilizes semiconductor quantum dots as luminescent materials to convert blue LED light into longer-wavelength red and green light. By adjusting the composition and size of the quantum dots, the emission wavelength can be precisely controlled,

H. Guo, J. He, J. Sun, Z. Huang, T. Guo, Q. Yan
College of Physics and Information Engineering
Fuzhou University
and Fujian Science & Technology Innovation Laboratory for
Optoelectronic Information of China
Fuzhou 350100, China
E-mail: jie.sun@fzu.edu.cn

K. Zhang
Fujian Key Laboratory of Agricultural Information Sensing Technology
College of Mechanical and Electrical Engineering
Fujian Agriculture and Forestry University
Fuzhou, Fujian 350002, China
E-mail: 958185645@qq.com

J. Sun
Department of Microscience and Nanotechnology
Chalmers University of Technology
Gothenburg 41296, Sweden

V. Belyaev, A. Abduev, A. Kazak
Federal State University of Education
Moscow 141014, Russia

**ADVANCED
SCIENCE NEWS**

www.advancedsciencenews.com

**ADVANCED
ELECTRONIC
MATERIALS**

www.advelectronicmat.de

enabling accurate color conversion. However, the poor stability of quantum dots may result in the degradation of their optical and chemical properties. The RGB combination method, on the other hand, involves transferring the Micro-LED chips of three colors onto a driving substrate using mass transfer technology to form a full-color pixel array. Although this method has significantly improved the resolution, yield, and production volume, it is difficult to achieve full-color Micro-LED displays with a pixel density greater than 1000 PPI.[16] Currently, full-color displays with pixel densities exceeding 1000 PPI are mostly realized through quantum dot color conversion. As a result, some researchers have turned to RGB chip stacking solutions. Compared to the color conversion and RGB combination methods, vertical stacking can reduce the area of a full-color pixel to at least one-third of that of a horizontal layout, thereby significantly increasing the pixel density of the display. In 2020, Li et al. developed a design based on stacked Micro-LED device arrays for full-color lighting and displays.[17] In 2023, Shin et al. reported a vertically stacked full-color Micro-LED using a 2D material layer transfer technique, achieving a pixel density of 5100 PPI.[16] In 2024, Li et al. developed a process for fabricating sidewall-insulated/uninsulated vias in the mesa gaps of Micro-LEDs.[18] The insulated vias are filled with SiO_2 to isolate different functional layers and prevent short circuits. The uninsulated vias are filled with metal to directly connect the anode of the Micro-LED to the complementary metal-oxide-semiconductor (CMOS) driving substrate. The R-G-B layers of the Micro-LED are electrically and mechanically connected through metal-filled vias by wafer bonding, enabling individual pixel control.

However, the increase in pixel density also exacerbates optical crosstalk between pixels. Simultaneously, as the size of Micro-LEDs continues to shrink, the proportion of sidewall area increases, leading to a higher proportion of sidewall emission.[19,20] Although sidewall emission enhances light extraction efficiency (LEE) to some extent, it exacerbates optical crosstalk and leads to non-uniform light intensity distribution among the RGB Micro-LEDs. This non-uniformity inevitably causes color shifts at different viewing angles when the Micro-LEDs are simultaneously illuminated, significantly degrading color consistency in high PPI displays.[21,22] To address the issues caused by sidewall emission, researchers have proposed various solutions, such as using photonic crystals,[23] patterned substrates,[24] and surface roughening[25] to disrupt total internal reflection (TIR) within Micro-LEDs and suppress sidewall emission. Alternatively, black matrices made of photoresist have been used to isolate subpixels and absorb sidewall emission.[26,27] However, there is limited research on suppressing sidewall emission in stacked Micro-LEDs. In addition, simply suppressing sidewall emission reduces the overall LEE. Therefore, there is an urgent need for a suitable design to suppress sidewall emission in stacked Micro-LEDs while maintaining high LEE.

Continuing the work of Li et al., who fabricated sidewall-insulated/uninsulated vias in the mesa gaps of Micro-LEDs, this study improves the design by replacing the metal pillars with metal walls through simulation. The cross-section of the metal wall is designed in an L-shape, with the vertical part embedded into the sidewall of the Micro-LED. Compared to metal pillars, the metal wall covers a larger sidewall area, providing better suppression of sidewall emission. The metal wall is made of Ag, a highly reflective metal, and the inclined sidewall and metal wall redirect the otherwise escaped light toward the top emission direction. This design achieves good electrical and mechanical connections between the Micro-LED and the CMOS driving substrate. More importantly, it significantly reduces sidewall emission (with a maximum reduction of 68.04%) while greatly enhancing top LEE (with a maximum increase of 196.18%). At the same time, it is believed that this work will be of great reference value for designing and fabricating vertically stacked RGB Micro-LEDs toward ultimately high PPI displays.

2. Design and Modeling

This device design includes Micro-LED models of three colors. The detailed design process is illustrated in **Figure 1a**, which consists of four simulation stages: parameter scanning, optimization of sidewall inclination angle, metal wall integration, and vertical stacking. First, parameter scanning is performed on Micro-LEDs of different sizes and epitaxial thicknesses to reveal the impact of these parameters on the Micro-LEDs. Next, the sidewalls of the Micro-LEDs are inclined, and the incline angle is optimized to improve the LEE and reshape the light distribution. Subsequently, an L-shaped metal wall is integrated into the inclined sidewalls to suppress sidewall emission and enhance top emission. Finally, the Micro-LEDs are vertically stacked, with the n-GaN surface of the blue Micro-LED serving as the light-emitting surface. The incline angle of the metal wall in each layer of the Micro-LED is optimized to improve LEE and light distribution. In the top view of Figure 1a, the white dashed line indicates the shape and position of the metal pillars. Compared to the metal pillars, the metal walls cover a larger sidewall area, thereby more effectively suppressing sidewall light emission. Figure 1b shows a 3D illustration of the electrode connections in the stacked Micro-LEDs, arranged from top to bottom as the red, green, and blue Micro-LEDs and the CMOS driving substrate. There are two reasons for designing this stacking method: 1) Given that the extinction coefficient of the MQW layer in the red Micro-LED is significantly large, the red Micro-LED is positioned at the bottom layer to ensure higher LEE for the green and blue Micro-LEDs. 2) Short wavelength light may excite the MQW layer of the Micro-LED, inducing photoluminescence, which could result in a color shift of the device. Consequently, the blue Micro-LED with the shortest wavelength emission is placed on the top layer, while the red Micro-LED with the longest wavelength emission is situated at the bottom layer. The electrical connection is established through the metal wall, which interfaces with the CMOS anode via insulated vias, and connects to the Micro-LED via bridge electrodes. The L-shaped metal wall also can serve as a common cathode for the RGB Micro-LEDs and the CMOS driving substrate. Figure 1c shows the equivalent circuit diagram.

Figure 2a shows the epitaxial structure of the GaN-based blue and green Micro-LEDs, which consists of a 0.1 µm ITO layer, a 0.1 µm p-GaN layer, a 0.1 µm multiple quantum well (MQW) layer, and a 1–6 µm n-GaN layer. Figure 2b shows the epitaxial structure of the AlGaInP-based red Micro-LED, which consists of a 0.1 µm ITO layer, a 0.1 µm p-AlGaInP layer, a 0.1 µm MQW layer, and a 1–6 µm n-AlGaInP layer. **Table 1** summarizes

ADVANCED
SCIENCE NEWS

www.advancedsciencenews.com
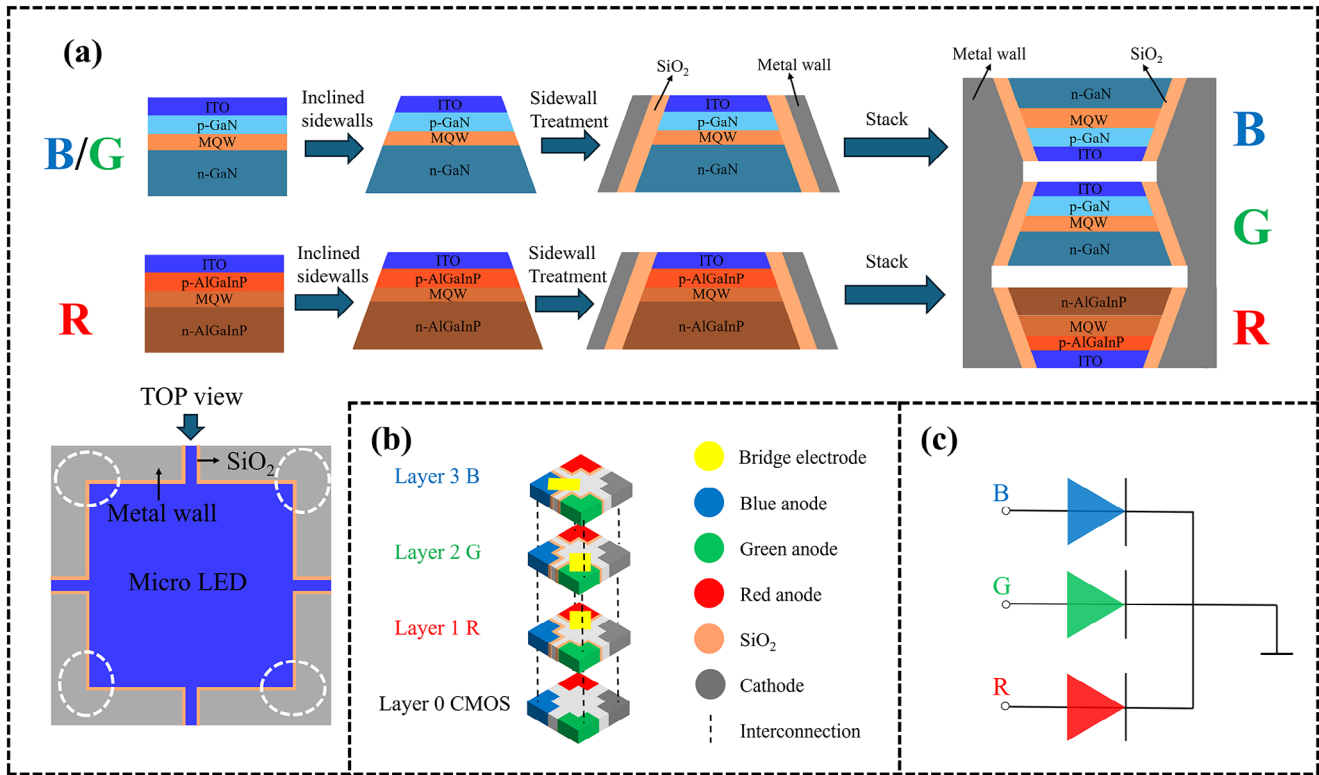
ADVANCED
ELECTRONIC
MATERIALS

www.advelectronicmat.de

Figure 1. a) Schematic diagram of the design process, and the white dashed line in the top view indicates the shape and position of the metal pillars. b) 3D illustration of the electrode connections in the stacked Micro-LEDs. c) Equivalent circuit diagram.
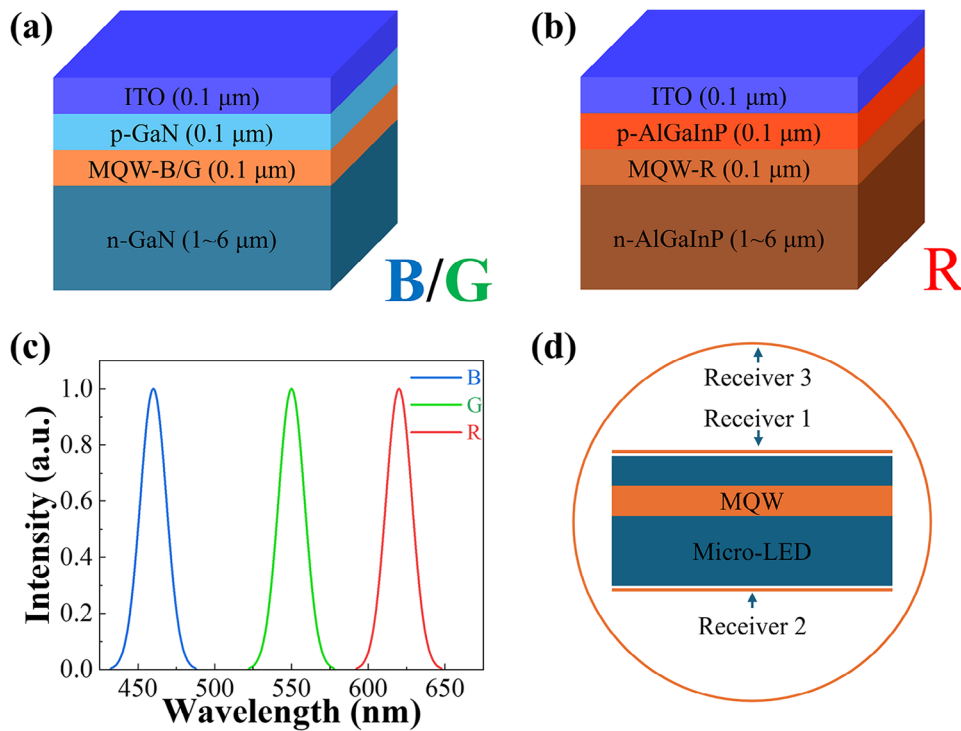

Figure 2. a) Epitaxial layer structure of the blue/green Micro-LEDs used in the simulation. b) The epitaxial layer structure of the red Micro-LED used in the simulation. c) Emission spectra of the Micro-LEDs used in the simulation. d) Receivers used in the simulation.

e70006 (3 of 11)

**ADVANCED
SCIENCE NEWS**

www.advancedsciencenews.com

**ADVANCED
ELECTRONIC
MATERIALS**

Open Access

www.advelectronicmat.de

Table 1. Refractive indices and extinction coefficients of the Micro-LED materials used in this study.

Layer	n [B/G/R]	k [B/G/R]	Layer	n [B/G/R]	k [B/G/R]
p/n-GaN	2.44/2.38/2.35	4e-5/4e-5/4e-5	ITO	1.96/1.86/1.80	0.0054/0.0032/0.0032
MQW-B/G	2.49/2.40/2.37	0.00196/4e-5/4e-5	p/n-AlGaInP	3.67/3.34/3.22	0.1573/0/0
MQW-R	4.09/3.73/3.64	0.49/0.25/0.176	SiO₂	1.47/1.47/1.46	0/0/0

the refractive indices and extinction coefficients of each epitaxial layer for the blue, green, and red wavelength bands. In this study, 3D ray-tracing method was employed for simulation to investigate the LEE and light distribution of the Micro-LEDs. The light source was positioned on the surface of the MQW layer. Figure 2c shows the emission spectra of the light sources used in this study. The central wavelengths of the red, green, and blue Micro-LEDs are 620 , 550 , and 460 nm, respectively, with a full width at half maximum (FWHM) of 20 nm for all. The radiant power of each light source was set to 1 watt. The detector configuration is shown in Figure 2d. Receiver 1 and Receiver 2 are planar detectors placed very close to the top and bottom surfaces of the Micro-LED, respectively, to collect light emitted from these surfaces. Receiver 3 is a far-field spherical detector that captures the overall light emitted by the Micro-LED. Based on this setup, the total LEE and sidewall emission LEE are defined as follows:

$$LEE_{Total} = \frac{P_{Receiver\,3}}{P_{Source}} \quad (1)$$

$$LEE_{Sidewall} = \frac{P_{Receiver\,3} - P_{Receiver\,2} - P_{Receiver\,1}}{P_{Source}} \quad (2)$$

3. Results and Discussion

3.1. Impact of Size and Epitaxial Thickness

The size of the Micro-LED has a significant impact on its LEE. In this study, parameter scanning was performed for single pixel RGB Micro-LEDs with sizes ranging from 16 to 96 μm in increments of 10 μm, and for n-GaN and n-AlGaInP thicknesses ranging from 1 to 6 μm in increments of 1 μm. **Figure 3** compares the LEE of Micro-LEDs with different sizes and epitaxial layer thicknesses. First, by comparing the LEE of the RGB Micro-LEDs, it is observed that the green Micro-LED exhibits the highest LEE, followed by the blue Micro-LED, while the red Micro-LED has the lowest LEE. This is due to the differences in the refractive indices of their epitaxial materials at different wavelengths. The refractive indices of GaN for blue and green light are 2.44 and 2.38, respectively, resulting in TIR angles of 24.19° and 25.77° for the blue and green Micro-LEDs. In contrast, AlGaInP has a refractive index of 3.22 for red light, leading to a TIR angle of only 18.09° for the red Micro-LED. Consequently, the green Micro-LED achieves the highest LEE, while the red Micro-LED has the lowest.

As the size of the Micro-LED increases, the optical path length for photons reaching the sidewalls increases, causing sidewall emission to gradually weaken and the total LEE to decrease, as shown in Figure 3. The thickness of the epitaxial layer has the most significant impact on the red Micro-LED, followed by the
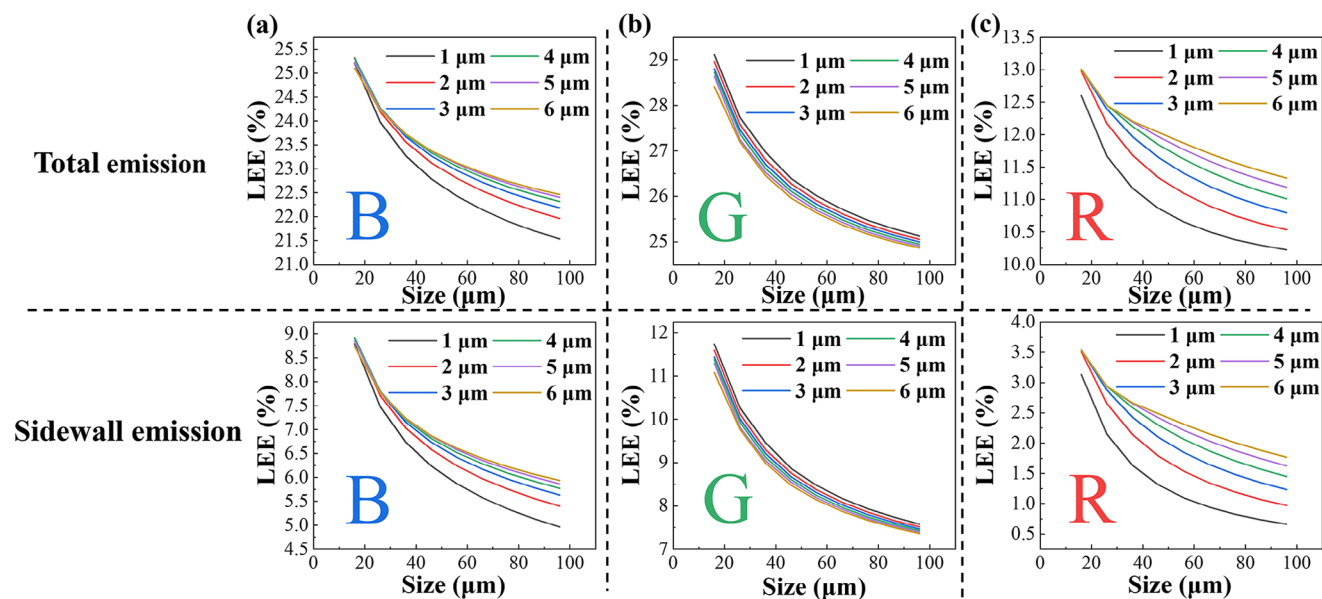

Figure 3. LEE variations of a) blue Micro-LEDs and b) green Micro-LEDs with different sizes under varying n-GaN thicknesses. c) LEE variations of red Micro-LEDs with different sizes under varying n-AlGaInP thicknesses.
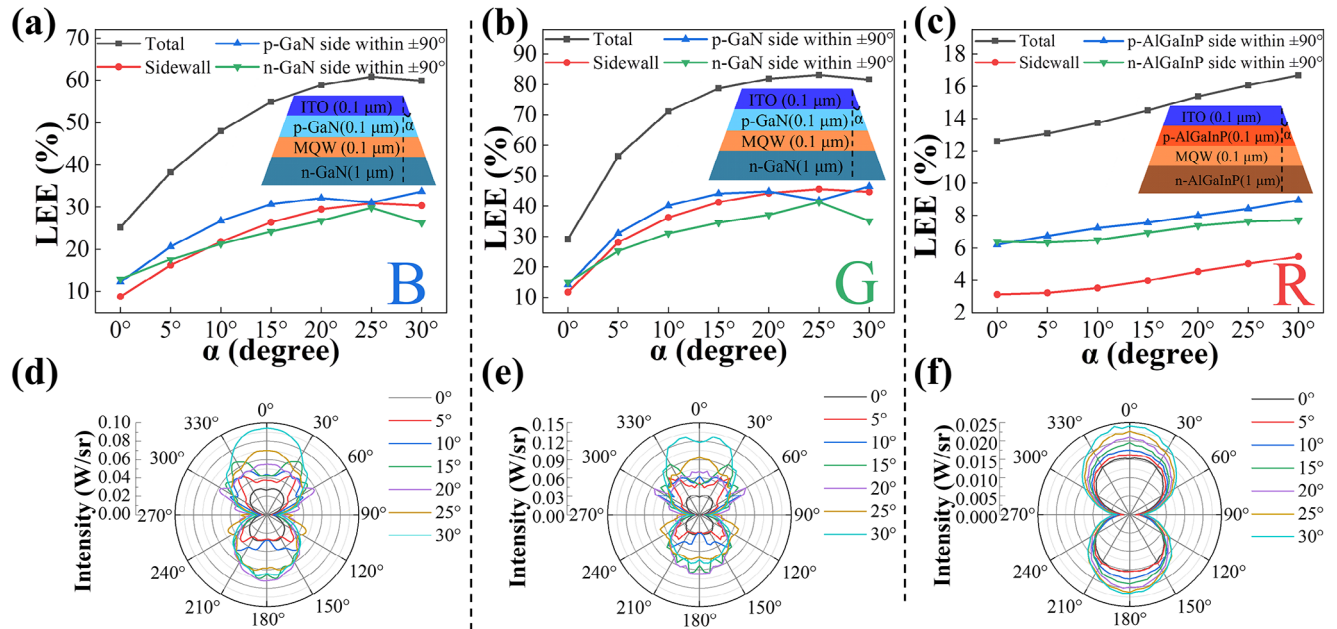
e70006 (4 of 11)

**ADVANCED
SCIENCE NEWS**

www.advancedsciencenews.com

**ADVANCED
ELECTRONIC
MATERIALS**

www.advelectronicmat.de

Figure 4. LEE diagrams of a) blue, b) green, and c) red Micro-LEDs at different incline angles. Light distribution diagrams of d) blue, e) green, and f) red Micro-LEDs at different incline angles.

blue Micro-LED. Thicker epitaxial layers result in more sidewall emission and an increase in total LEE, as shown in Figure 3a,c. However, the impact of epitaxial layer thickness on the green Micro-LED is less pronounced compared to the red and blue Micro-LEDs, and its effect on LEE is opposite to that observed for the red and blue Micro-LEDs, as shown in Figure 3b. To achieve higher LEE and smaller device size, a Micro-LED with dimensions of 16 μm × 16 μm and an epitaxial layer thickness of 1.3 μm was selected. Subsequently, optimizations were performed sequentially, including sidewall incline angle optimization, metal wall integration, and vertical stacking.

3.2. Inclined Sidewall Optimization

Inclined sidewalls are a highly effective method for improving LEE, and they also facilitate the reflection of sidewall-emitted light back to the top emission direction by the metal wall. To validate the positive effects of the metal wall on the LEE and light distribution of Micro-LEDs, this study sampled the incline angles of the Micro-LED sidewalls for subsequent comparison. Considering the feasibility in practical fabrication, the incline angle α was varied from 0° to 30° in increments of 5° for simulation.

Figure 4a shows that the total LEE and the sidewall LEE of blue Micro-LED gradually increase with the incline angle, but the rate of improvement slows down, reaching a maximum at 25° with a total LEE improvement of 147.37% compared to the vertical sidewall. The LEE within ±90° on the n-GaN side is higher than that on the p-GaN side at $\alpha = 0°$, but it becomes lower than the p-GaN side after sidewall inclination. At $\alpha = 25°$, the n-GaN side achieves the maximum LEE within ±90°, which is 129.76% higher than that of the vertical sidewall. The p-GaN side LEE within ±90° reaches its maximum at 30°, showing a 175% im-

provement compared to the vertical sidewall. Figure 4d shows the light distribution of the blue Micro-LED. When $\alpha = 0°$, the light intensity in the lower half of the polar coordinate is significantly higher than that in the upper half. As the angle increases, the light intensity in the upper half steadily increases, while the increase in the lower half is less pronounced, consistent with the LEE trends.

Figure 4b shows that the LEE trends of the green Micro-LED are similar to those of the blue Micro-LED. The total LEE reaches its maximum at $\alpha = 25°$, with an improvement of 185.44% compared to the vertical sidewall. At $\alpha = 25°$, the n-GaN side achieves the maximum LEE within ±90°, which is 176.14% higher than that of the vertical sidewall. The p-GaN side LEE within ±90° reaches its maximum at $\alpha = 30°$, showing a 195.48% improvement compared to the vertical sidewall. The light distribution of the green Micro-LED also follows a similar trend to that of the blue Micro-LED, as shown in Figure 4e.

Figure 4c shows that the total LEE, the sidewall LEE, and p-AlGaInP side LEE within ±90° of the red Micro-LED all increase with α. However, the n-AlGaInP side LEE within ±90° slightly decreases at $\alpha = 5°$ before gradually increasing. The total LEE, p-AlGaInP side LEE within ±90°, and n-AlGaInP side LEE within ±90° all reach their maximum values at $\alpha = 30°$, with improvements of 32.38%, 44.12%, and 20.81%, respectively, compared to the vertical sidewall. The light distribution of the red Micro-LED exhibits a Lambertian-like distribution at all incline angles, and the trends in light distribution align with the LEE trends, as shown in Figure 4f. The impact of inclined sidewalls on the red Micro-LED is significantly smaller than that on the blue and green Micro-LEDs. This is due to the high extinction coefficient of the MQW layer, which prevents most light from escaping through the sidewalls or top. Additionally, the large refractive index difference between the red
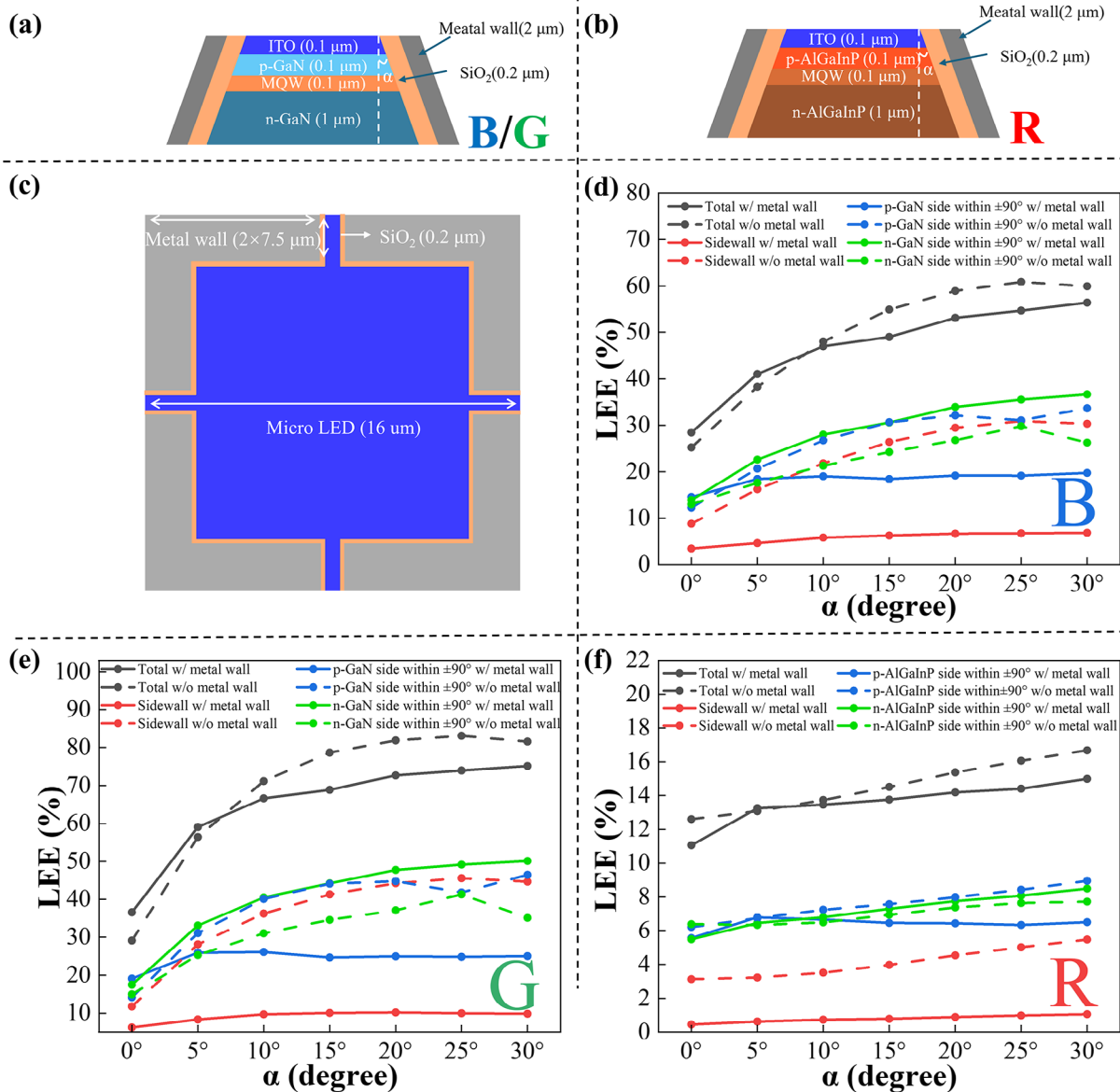
**ADVANCED
SCIENCE NEWS**

www.advancedsciencenews.com

**ADVANCED
ELECTRONIC
MATERIALS**

www.advelectronicmat.de

Figure 5. Structural diagrams of a) blue, green, and b) red Micro-LEDs with metal walls. c) Top view of a Micro-LED with a metal wall. Comparison of LEE for d) blue, e) green, and f) red Micro-LEDs with and without metal walls.

Micro-LED chip and air results in a very small TIR angle, which is another critical factor. Furthermore, the epitaxial wafers of blue and green Micro-LEDs are composed of InGaN/GaN MQW, while the epitaxial wafers of red Micro-LEDs are composed of GaInP/AlGaInP MQW. These differences further exacerbate the situation where the emission patterns of RGB Micro-LEDs vary considerably.

3.3. L-Shaped Metal Wall Integration

Although the inclined sidewall method can significantly improve the LEE of Micro-LEDs, most of the LEE improvement comes from the sidewalls. To suppress sidewall emission and reuse

the light, we designed an L-shaped metal wall structure on the sidewalls, as shown in **Figure** 5a–c. The metal wall is made of Ag.

From Figure 5d, which compares the LEE of the blue Micro-LED with and without the metal wall, it is evident that the metal wall has a significant impact on LEE. The metal wall effectively suppresses sidewall emission, and at $\alpha = 0°$ and $\alpha = 5°$, not only is sidewall emission reduced, but the total LEE is also enhanced. At $\alpha = 25°$, the reduction in sidewall emission reaches its maximum of 78.19%, while the total LEE only decreases by 10.16%. Although the total LEE decreases after $\alpha = 5°$, analyzing the LEE on the n-GaN and p-GaN sides separately reveals that the metal wall redirects light originally emitted through the sidewalls on the p-GaN side back to the n-GaN side. This results in an increase
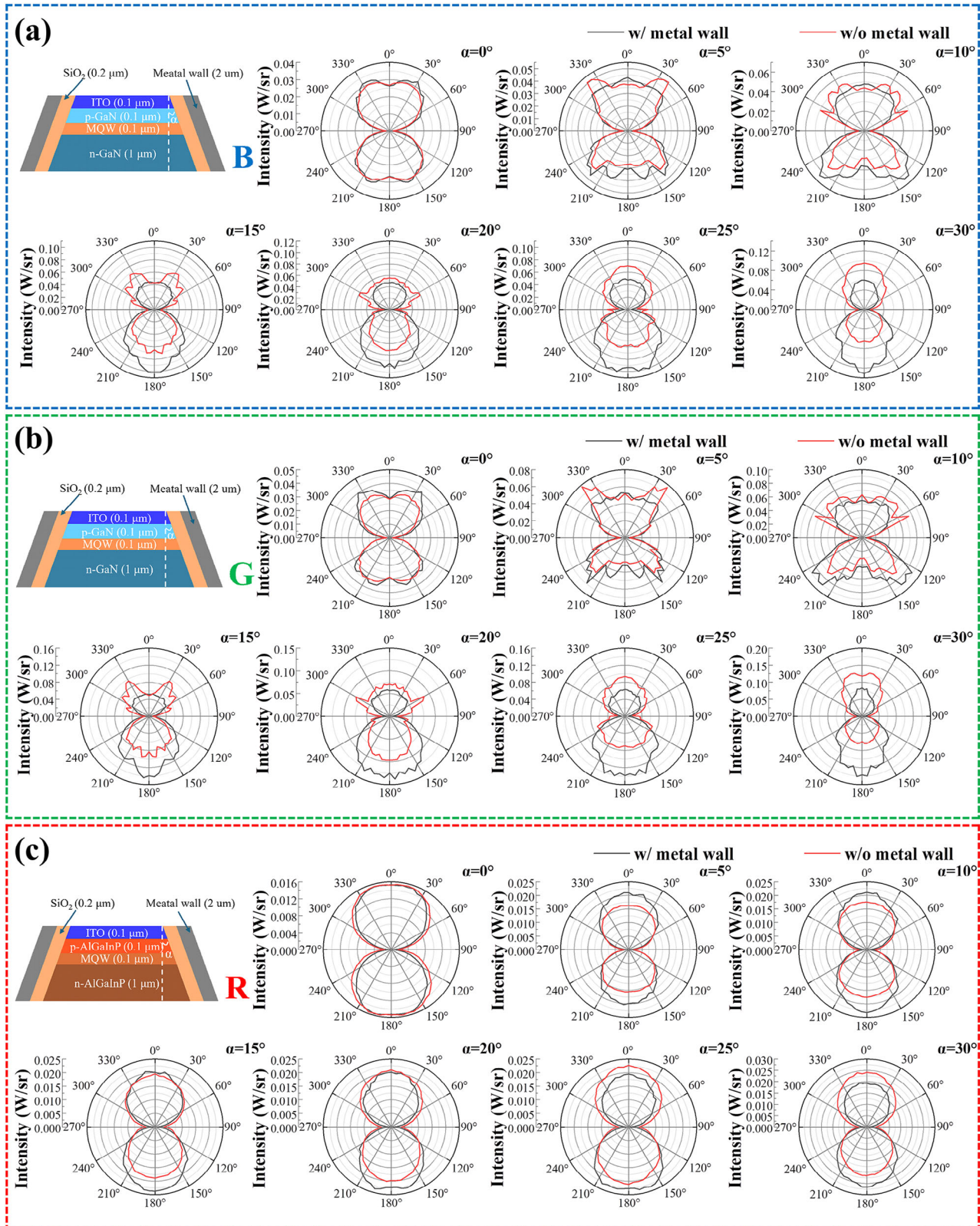
e70006 (6 of 11)

Figure 6. Comparison of light distribution for a) blue, b) green, and c) red Micro-LEDs with and without metal walls at inclined sidewall angles of 0°–30°.

**ADVANCED
SCIENCE NEWS**

www.advancedsciencenews.com

**ADVANCED
ELECTRONIC
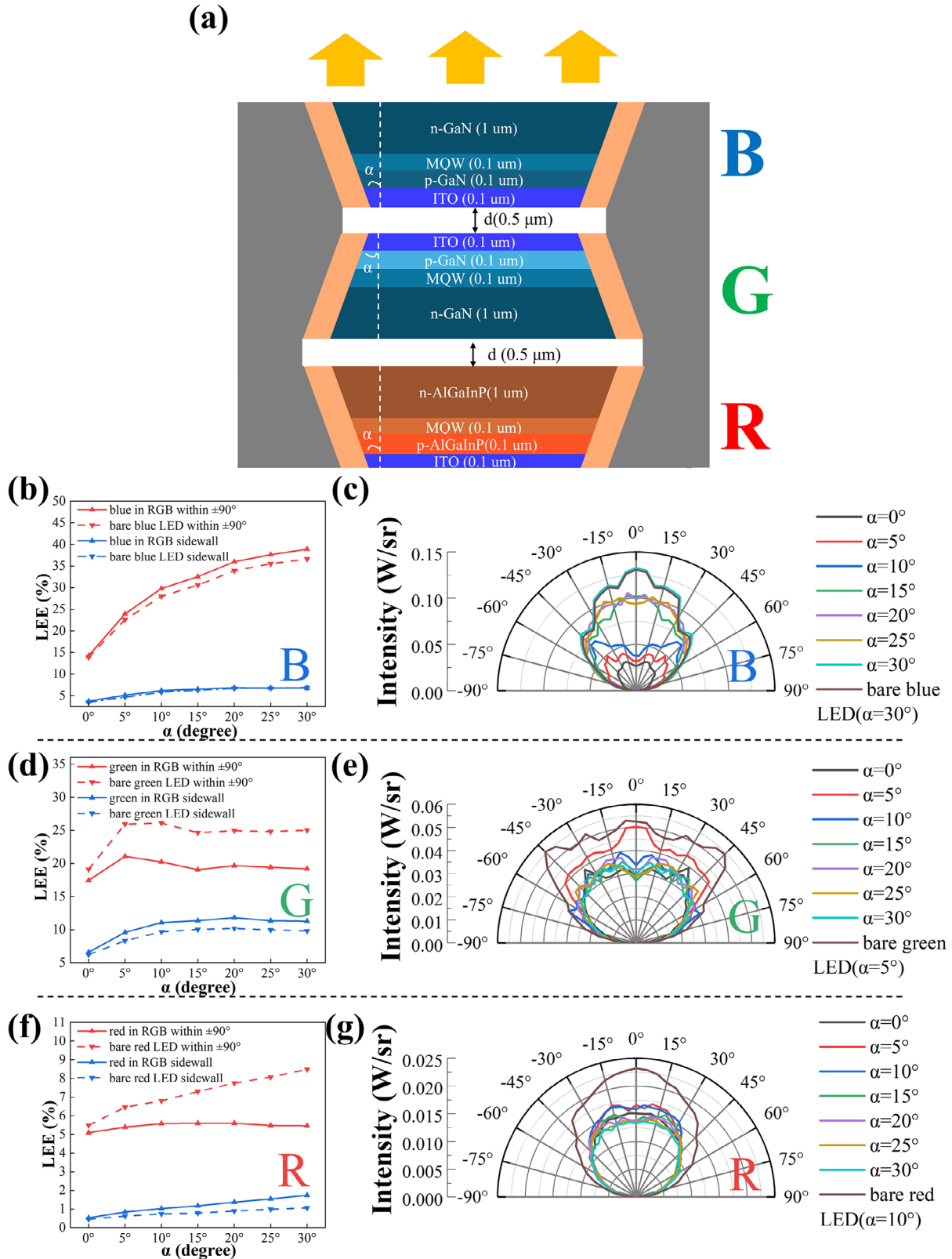MATERIALS**
Open Access

www.advelectronicmat.de

Figure 7. a) Structure diagram of vertically stacked Micro-LEDs with L-shaped metal walls. b) LEE and c) light distribution diagrams of blue Micro-LEDs at different incline angles after vertical stacking. d) LEE and e) light distribution diagrams of green Micro-LEDs at different incline angles after vertical stacking. f) LEE and g) light distribution diagrams of red Micro-LEDs at different incline angles after vertical stacking.
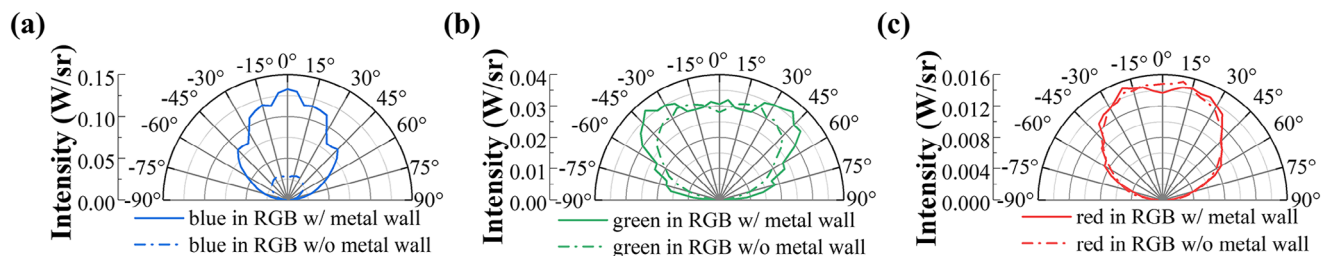
e70006 (8 of 11)

**ADVANCED
SCIENCE NEWS**

www.advancedsciencenews.com

**ADVANCED
ELECTRONIC
MATERIALS**

www.advelectronicmat.de

Figure 8. Comparison of light distribution between vertically stacked Micro-LEDs with and without L-shaped metal walls for a) blue, b) green, and c) red light.

in the LEE within $\pm90°$ on the n-GaN side and a decrease on the p-GaN side. At $\alpha = 30°$, the LEE within $\pm90°$ on the n-GaN side reaches its maximum, showing a 39.53% increase compared to the case without the metal wall. The increase in light emission from the n-GaN side and the decrease from the p-GaN side are beneficial for subsequent flip-chip bonding.

From Figure 5e, which compares the LEE of the green Micro-LED with and without the metal wall, the trends are consistent with those of the blue Micro-LED. The metal wall suppresses sidewall emission and even increases the total LEE at $\alpha = 0°$ and $\alpha = 5°$. At $\alpha = 25°$, the reduction in sidewall emission reaches its maximum of 78.14%, while the total LEE only decreases by 11%. As the incline angle α increases, the light emission from the p-GaN side decreases compared to the case without the metal wall, while the light emission from the n-GaN side increases. The magnitude of these changes grows with the inclined angle. At $\alpha = 30°$, the LEE within $\pm90°$ on the n-GaN side achieves a maximum increase of 42.7%.

From Figure 5f, which compares the LEE of the red Micro-LED with and without the metal wall, the metal wall also suppresses sidewall emission in the red Micro-LED. At $\alpha = 30°$, the reduction in sidewall emission reaches its maximum of 80.66%, while the total LEE only decreases by 10.12%. Although the total LEE decreases after $\alpha = 5°$, analyzing the LEE within $\pm90°$ on the n-AlGaInP and p-AlGaInP sides separately reveals that, similar to the blue and green Micro-LEDs, the metal wall redirects light originally emitted through the sidewalls on the p-AlGaInP side back to the n-AlGaInP side. This results in an increase in the LEE within $\pm90°$ on the n-AlGaInP side and a decrease on the p-AlGaInP side. At $\alpha = 30°$, the LEE within $\pm90°$ on the n-AlGaInP side achieves a maximum increase of 9.97%.

Figure 6a shows the comparison of light distribution for the blue Micro-LED with inclined sidewalls at $\alpha = 0°-30°$. At $\alpha =$

0°, the light reflected by the metal wall is emitted from both the top and bottom surfaces of the Micro-LED, slightly increasing the light intensity. As the angle α increases, the metal wall, which is inclined downward, reflects more light from the sidewalls to the n-GaN side, thereby reducing light emission from the p-GaN side and enhancing emission from the n-GaN side. The larger the incline angle, the more pronounced the enhancement of light emission from the n-GaN side. This is consistent with the LEE analysis in Figure 5d. The angle α also affects the FWHM of the light pattern. As α increases, the FWHM on the n-GaN side initially increases and then decreases.

The changes in light distribution for the green Micro-LED with inclined sidewalls at $\alpha = 0°-30°$ are consistent with those of the blue Micro-LED. At $\alpha = 0°$, the metal wall enhances light emission from both the top and bottom sides of the Micro-LED. As the angle α increases, light emission from the p-GaN side decreases, while emission from the n-GaN side increases, as shown in Figure 6b.

The light distribution of the red Micro-LED differs from that of the blue and green Micro-LEDs. After adding the metal wall, the light distribution of the red Micro-LED remains Lambertian-like, as shown in Figure 6c. At $\alpha = 5°-15°$, the metal wall enhances light emission from both the top and bottom sides of the red Micro-LED, but the degree of enhancement gradually decreases. At $\alpha = 15°-30°$, the metal wall reduces light emission from the p-AlGaInP side and enhances emission from the n-AlGaInP side. This observation is inconsistent with the LEE analysis of the red Micro-LED in Figure 5f. The discrepancy arises because the light distribution diagram represents optical data from a 2D cross-section within a 3D space, whereas LEE is calculated based on the entire 3D space. Therefore, even if a structure has a higher LEE value, it does not necessarily mean that its light distribution is superior in every cross-section.

Table 2. Performance comparison between vertically stacked Micro-LEDs with and without L-shaped metal walls.

Type	LEE of sidewall emission [%]	Decrease	LEE within $\pm90°$ [%]	Increase
Blue in RGB w/o metal wall	8.67	20.30%	13.08	196.18%
Blue in RGB w/ metal wall	6.91		38.74	
Green in RGB w/o metal wall	11.79	16.54%	12.75	51.69%
Green in RGB w/ metal wall	9.84		19.34	
Red in RGB w/o metal wall	3.16	68.04%	5.21	3.45%
Red in RGB w/ metal wall	1.01		5.39	

3.4. Vertical Stacking Performance

Next, we discuss the effects of the vertically stacked RGB Micro-LEDs with L-shaped metal walls. **Figure** 7a shows the structure of the vertically stacked Micro-LEDs with L-shaped metal walls, where the pixel pitch d is 0.5 µm, and the light-emitting surface is the n-GaN side of the blue Micro-LED. Figure 7b illustrates the variation in the LEE of the blue Micro-LED at different incline angles after vertical stacking. The LEE trend of the vertically stacked blue Micro-LED is consistent with that of the single pixel case, increasing as the angle α increases. Due to the reflection from the metal walls of the green and red Micro-LEDs, the LEE within ±90° on the light-emitting surface is slightly higher than that of the single pixel case. Additionally, because light also escapes from the gaps between pixels, the sidewall LEE is slightly higher compared to the single pixel case. However, since the blue Micro-LED is located at the top of the stacked structure, its light distribution is less affected by the underlying layers. The light distribution diagram provides a more intuitive view of the changes in light intensity with angle and before/after vertical stacking. At α = 30°, the light intensity reaches its maximum, with a 6.17% increase compared to the single pixel case, as shown in Figure 7c.

Figure 7d shows the variation in the LEE of the green Micro-LED at different incline angles after vertical stacking. The LEE trend of the vertically stacked green Micro-LED is consistent with that of the single pixel case. Unlike the blue Micro-LED, the green Micro-LED experiences a significant reduction in the LEE within ±90° on the light-emitting surface after vertical stacking due to the TIR reflection from both the green and blue Micro-LED layers. The sidewall LEE also increases compared to the single pixel case because light escapes from the gaps between pixels. The light distribution diagram in Figure 7e visually reflects the LEE trends shown in Figure 7d. At α = 5°, the vertically stacked green Micro-LED achieves its maximum light intensity, which is 18.77% lower than that of the single pixel green Micro-LED at α = 5°.

Figure 7f shows the variation in the LEE of the red Micro-LED at different incline angles after vertical stacking. After vertical stacking, the LEE within ±90° on the light-emitting surface of the red Micro-LED is less affected by the angle, showing a trend of initially increasing and then decreasing with angle. The larger the angle, the greater the reduction compared to the single pixel case. The sidewall LEE increases with the angle, and due to light escaping from the gaps between pixels, it is also higher than that of the single pixel case. Figure 7g shows the light distribution of the vertically stacked red Micro-LED at different incline angles. The light intensity reaches its maximum at α = 10°, which is 17.91% lower than that of the single pixel red Micro-LED at α = 10°.

To validate the performance improvement of vertically stacked Micro-LEDs with L-shaped metal walls, a simulation comparison was conducted between vertically stacked Micro-LEDs with and without L-shaped metal walls. Based on the analysis of Figure 7, the incline angles for the red, green, and blue Micro-LEDs in the L-shaped metal wall structure were selected as 10°, 5°, and 30°, respectively, to ensure the highest LEE, while the vertically stacked Micro LED without metal walls has vertical sidewalls. By combining **Figure 8** and **Table** 2, we can clearly observe the optimization effect of the L-shaped metal wall on the performance of vertically stacked Micro-LEDs. For the blue Micro-LED with L-shaped metal walls, the LEE within ±90° on the light-emitting surface increased by 196.18%, while the sidewall LEE decreased by 20.30% compared to the structure without metal walls. For the green Micro-LED, the LEE within ±90° on the light-emitting surface increased by 51.69%, and the sidewall LEE decreased by 16.54%. For the red Micro-LED, the LEE within ±90° on the light-emitting surface increased by 3.45%, and the sidewall LEE decreased by 68.04%.

4. Conclusion

In this study, by introducing an L-shaped metal wall structure and inclined sidewall design, we suppressed sidewall emission and significantly improved the LEE of vertically stacked Micro-LEDs while achieving electrical and mechanical connections between the vertically stacked Micro-LEDs and the CMOS driving substrate. The L-shaped metal wall effectively reduces sidewall emission by reflecting sidewall light toward the top emission direction (the sidewall LEE of the red Micro-LED is reduced by 68.04% compared to conventional vertical stacking). It also significantly enhances top light intensity (the LEE within ±90° for blue and green Micro-LEDs is increased by 196.18% and 51.69%, respectively, compared to conventional vertical stacking), while the red Micro-LED maintains its Lambertian-like distribution characteristics. This study provides a theoretical foundation and technical pathway for the industrialization of full-color Micro-LED displays. However, the research is based on idealized simulation conditions. Future work should include experimental validation of the process compatibility of the metal wall structure and further performance improvements through optimization of metal wall materials and stacking processes, thereby advancing the development of high-resolution display technologies.

Conflict of Interest

The authors declare no conflict of interest.

Data Availability Statement

The data that support the findings of this study are available from the corresponding author upon reasonable request.

**ADVANCED
SCIENCE NEWS**

www.advancedsciencenews.com

**ADVANCED
ELECTRONIC
MATERIALS**
Open Access

www.advelectronicmat.de

[1] L. H. Qi, X. Zhang, W. C. Chong, P. A. Li, K. M. Lau, *Opt. Express* **2021**, *29*, 10580.

[2] Y. F. Wu, J. S. Ma, P. Su, L. J. Zhang, B. Z. Xia, *Nanomaterials* **2020**, *10*, 2482.

[3] Z. T. Ye, L. Wei, C. H. Tien, S. M. Pan, *Opt. Express* **2022**, *30*, 13447.

[4] J. F. C. Carreira, E. Xie, R. Bian, C. Chen, J. J. D. McKendry, B. Guilhabert, H. Haas, E. Gu, M. D. Dawson, *Opt. Express* **2019**, *27*, A1517.

[5] Y. Huang, G. Tan, F. Gou, M. C. Li, S. L. Lee, S. T. Wu, *J. Soc. Inf. Display.* **2019**, *27*, 387.

[6] T. Zhan, K. Yin, J. H. Xiong, Z. Q. He, S. T. Wu, *Iscience* **2020**, *23*, 101397.

[7] H. Yu, M. H. Memon, D. Wang, Z. Ren, H. Zhang, C. Huang, M. Tian, H. Sun, S. Long, *Opt. Lett.* **2021**, *46*, 3271.

[8] H. Yu, J. Yao, M. H. Memon, Y. Luo, Z. Gao, D. Luo, R. Wang, Z. Wang, W. Chen, L. Wang, S. Li, J. Zheng, J. Zhang, S. Liu, H. Sun, *Laser Photonics Rev.* **2025**, *19*, 2401220.

[9] H. Yu, S. Xiao, M. H. Memon, Y. Luo, R. Wang, D. Li, C. Shen, H. Sun, *Laser Photonics Rev.* **2024**, *18*, 2300789.

[10] Y. G. Huang, E. L. Hsiang, M. Y. Deng, S. T. Wu, *Light-Sci. Appl.* **2020**, *9*, 105.

[11] D. Park, Y. Jeong, Y. Moon, Y. Park, *Displays* **2023**, *79*, 102498.

[12] B. R. Hyun, C. W. Sher, Y. W. Chang, Y. H. Lin, Z. J. Liu, H. C. Kuo, *J. Phys. Chem. Lett.* **2021**, *12*, 6946.

[13] H. V. Han, H. Y. Lin, C. C. Lin, W. C. Chong, J. R. Li, K. J. Chen, P. C. Yu, T. M. Chen, H. M. Chen, K. M. Lau, H. C. Kuo, *Opt. Express* **2015**, *23*, 32504.

[14] F. W. Gou, E. L. Hsiang, G. J. Tan, Y. F. Lan, C. Y. Tsai, S. T. Wu, *Crystals* **2019**, *9*, 39.

[15] A. R. Anwar, M. T. Sajjad, M. A. Johar, C. A. Hernández-Gutiérrez, M. Usman, S. P. Łepkowski, *Laser Photonics Rev.* **2022**, *16*, 2100427.

[16] J. Shin, H. Kim, S. Sundaram, J. Jeong, B. I. Park, C. S. Chang, J. Choi, T. Kim, M. Saravanapavanantham, K. Y. Lu, S. Kim, J. M. Suh, K. S. Kim, M. K. Song, Y. P. Liu, K. Qiao, J. H. Kim, Y. Kim, J. H. Kang, J. Kim, D. Lee, J. Lee, J. S. Kim, H. E. Lee, H. Yeon, H. S. Kum, S. H. Bae, V. Bulovic, K. J. Yu, K. Lee, et al., *Nature* **2023**, *614*, 81.

[17] L. Z. Li, G. Tang, Z. Shi, H. Ding, C. B. Liu, D. L. Cheng, Q. Y. Zhang, L. Yin, Z. B. Yao, L. Duan, D. H. Zhang, C. G. Wang, M. X. Feng, Q. Sun, Q. Wang, Y. J. Han, L. Wang, Y. Luo, X. Sheng, *Proc. Natl. Acad. Sci. USA* **2021**, *118*, 2023436118.

[18] Y. Li, K. X. Zhang, T. X. Yang, J. Y. Nie, Q. W. Li, Y. J. Zhou, T. Tao, T. Zhi, Q. Yan, J. Sun, *Opt. Commun.* **2025**, *575*, 131332.

[19] J. Y. Kim, J. R. Park, M. K. Kwon, *J. Nanosci. Nanotechno.* **2019**, *19*, 2346.

[20] J. Q. Kou, C. C. Shen, H. Shao, J. M. Che, X. Hou, C. S. Chu, K. K. Tian, Y. H. Zhang, Z. H. Zhang, H. C. Kuo, *Opt. Express* **2019**, *27*, A643.

[21] Y. Liu, T. Xia, A. Du, T. Liang, Z. Fan, E. Chen, J. Sun, Q. Yan, T. Guo, *Opt. Lett.* **2023**, *48*, 1650.

[22] S.-W. H. Chen, Y.-M. Huang, K. J. Singh, Y.-C. Hsu, F.-J. Liou, J. Song, J. Choi, P.-T. Lee, C.-C. Lin, Z. Chen, J. Han, T. Wu, H.-C. Kuo, *Photonics. Res.* **2020**, *8*, 630.

[23] S. Lan, H. Wan, J. Zhao, S. Zhou, *Micromachines* **2019**, *10*, 860.

[24] S. M. Yang, C. H. Chao, Y. S. Chen, M. H. Wu, Y. H. Fang, C. C. Lin, *Appl. Opt.* **2024**, *63*, 2503.

[25] B. K. Saifaddin, M. Iza, H. Foronda, A. Almogbel, C. J. Zollner, F. Wu, A. Alyamani, A. Albadri, S. Nakamura, S. P. DenBaars, J. S. Speck, *Opt. Express* **2019**, *27*, A1074.

[26] F. W. Gou, E. L. Hsiang, G. J. Tan, P. T. Chou, Y. L. Li, Y. F. Lan, S. O. Wu, *Opt. Express* **2019**, *27*, A746.

[27] X. Zhang, A. L. Chen, T. Yang, J. H. Cai, Y. Y. Ye, E. G. Chen, S. Xu, Y. Ye, J. Sun, Q. Yan, T. L. Guo, *IEEE Photonics J.* **2022**, *14*, 7014207.

e70006 (11 of 11)